

The Kinetics of the Chlorination of Yttrium Oxide

J.P. GAVIRÍA and A.E. BOHÉ

The chlorination kinetics of Y_2O_3 with chlorine to produce $YOCl$ was studied by thermogravimetry over a temperature range from 575 °C to 975 °C. The influence of convective mass transfer into the boundary layer surrounding the sample, gaseous diffusion into the sample pores, partial pressure of chlorine, and temperature on the reaction rate were analyzed in order to determine the rate-controlling step. The thermogravimetric and scanning electron microscopy (SEM) results showed that the process follows a model of nucleation and growth, and the process is chemically controlled for temperatures lower than 800 °C, with an activation energy (E_a) of 187 ± 3 kJ/mol. In the 850 °C to 975 °C range the reaction rate was affected by diffusion of Cl_2 through the gas film surrounding the sample, with apparent E_a of 105 ± 11 kJ/mol.

A global rate equation that includes these parameters has been developed $R = d\alpha/dt = 10^5 \text{ kPa}^{-1} \cdot \exp\left(-\frac{187 \text{ kJ}\cdot\text{mol}^{-1}}{R\cdot T}\right) \cdot pCl_2 \cdot 1.51 \cdot (1 - \alpha) \cdot [-\ln(1 - \alpha)]^{0.34}$

DOI: 10.1007/s11663-008-9215-x

© The Minerals, Metals & Materials Society and ASM International 2009

I. INTRODUCTION

YTTRIUM oxide is one of the most important compounds of yttrium and is widely used in many ceramic materials. The chlorination process is a potential dry method of production of the rare earth chlorides as precursors, which allow the isolation of metals from ores and concentrates, refining metals and recovering metals from slags, besides having application in advanced ceramic areas.^[1] The group called rare earth elements (REE) denotes the group of 17 chemically similar metallic elements that includes Sc, Y, and Lanthanides. The Lanthanides are composed by the series of elements with atomic numbers between 51 and 71.^[2] The REE are chemically similar to one another, and invariably occur together in the source minerals and behave as a single chemical entity. On the basis of their separability, the REE group has been divided into the “cerium group” or “light REE” (La to Eu) and the “yttrium group” or “heavy group” (Gd to Lu plus Y). They are not present as high-grade ore; the only REE and Y minerals of commercial interest are monazite, bastnaesite, and xenotime. The first two contain predominantly light rare earths, whereas xenotime is rich in heavy rare earths.^[3] The separation of each element is mainly based on three methods:^[4] the reduction of the

anhydrous chloride, the reduction of the oxide, and the electrolysis of the fused salt. So, it is very important to study the synthesis and kinetics of formation of the rare earth chlorides.

Although there are many studies concerning the chlorination of REE, few studies have been concerned with the kinetics, mechanism, and structural changes involved in the direct chlorination. Gimenes *et al.*^[1] focused their investigation on the reaction between xenotime ($REEPO_4$) and chlorine in the presence of carbon over a temperature range from 600 °C to 950 °C, as well as the microstructural changes occurring during the reaction. They found that yttrium oxychloride ($YOCl$) was produced in an intermediary step during the carbochlorination of the xenotime ore, and then the reaction could be followed by a fast step related to the generation of the yttrium trichloride (YCl_3). Augusto *et al.*^[5] investigated the kinetics of chlorination and microstructural changes of xenotime by carbon tetrachloride at temperatures from 600 °C to 900 °C. Their results showed that the reaction follows the shrinking-unreacted-core model with formation of a product layer ($YOCl$), which is chlorinated to give YCl_3 . Braginski *et al.*^[6] studied the chlorination of yttrium oxide in the presence of carbon at 1100 °C. They concluded that the reaction proceeds *via* two stages. The first one called “incubation period” which leads to the formation of $YOCl$ as the major reaction product. With progressing chlorination, YCl_3 is formed in a second stage.

The purpose of this work is to study the kinetics of the direct chlorination of yttrium oxide in order to determine the rate equation, elucidate the reaction stages, and obtain kinetics parameters. The technique used to follow the course of the reaction was an electrobalance and the solids were analyzed by X-ray diffraction (XRD), scanning electron microscopy (SEM), energy dispersive spectroscopy (EDS), laser diffraction (particle size distribution), and nitrogen adsorption technique (BET area).

J.P. GAVIRÍA, PhD Student, is with the Instituto de Energía y Desarrollo Sustentable - Centro Atómico Bariloche - Comisión Nacional de Energía Atómica, Av. Bustillo 9500 (8400), S.C. de Bariloche, Río Negro Argentina, Argentina, and Consejo Nacional de Investigaciones Científicas y Técnicas, Buenos Aires, Argentina. A.E. BOHÉ, Researcher, is with the Instituto de Energía y Desarrollo Sustentable - Centro Atómico Bariloche - Comisión Nacional de Energía Atómica, Consejo Nacional de Investigaciones Científicas y Técnicas, and Centro Regional Universitario Bariloche, Universidad Nacional del Comahue, Comahue, Argentina. Contact e-mail: gavirij@cab.cnea.gov.ar

Manuscript submitted April 23, 2008.

Article published online January 13, 2009.

II. EXPERIMENTAL SECTION

A. Materials

Solid reactant used was an yttrium oxide powder 99.99 pct (Aldrich Chemical Company, Inc., Milwaukee, MI). Gases used were Cl₂ 99.8 pct purity (Indupa, Bahia Blanca, Argentina) and Ar 99.99 pct purity (AGA, Buenos Aires, Argentina). The mean particle size measured by laser diffraction was 10 μm and showed a size distribution highly homogeneous (Mastersizer, Malvern Instruments Limited, Worcestershire, UK). The powder has a BET area of 3.7 m²/g (Digisorb 2600 Micromeritics Instrument, Norcross, GA).

B. Thermogravimetric System

Mass change occurring during the Y₂O₃ chlorination was measured using a thermogravimetric analyzer (TGA), which has been described elsewhere.^[7] It consists of an electrobalance (model 2000, Cahn Instruments, Inc., Cerritos, CA) adapted for working with corrosive atmospheres, a vertical tube furnace, a gas line, and a data acquisition system. This experimental setup has a sensitivity of ±5 μg while operating at 1000 °C under a gas flow rate of 9 L/h, measured at normal temperature and pressure. Each sample was placed in a cylindrical quartz crucible (7.8-mm inner diameter, 3.3-mm deep), which hangs from one of the arms of the electrobalance through a quartz wire. A quartz hangdown tube (4.6-cm diameter) carried the gases to the sample. The temperature of the sample was measured using a Pt-Pt (10 pct Rh) thermocouple encapsulated in quartz, which was placed 2 mm below the crucible. Flows of Ar and Cl₂ gases were controlled by means of flow meters and they were dried by passing through silica gel and CaCl₂, respectively. The mass changes monitored with this experimental setup were acquired every 2.5 seconds using the data acquisition system.

C. Procedure

Nonisothermal and isothermal runs were performed. In the first runs, samples were kept 1 h under flowing Ar to purge the gas line and heated at 100 °C to eliminate water. Then the chlorine gas was injected at that temperature and samples were heated in the Ar-Cl₂ mixture up to 950 °C. The linear heating rate used was 3.8 °C/min. Mass changes were continuously monitored during the heating, and the apparent mass change was taken into account to correct the experimental data.^[7] In the isothermal experiments, samples were heated in flowing Ar to the selected reaction temperature. After the temperature was stabilized, chlorine was admitted into the hangdown tube while mass changes were continuously monitored. The data were carefully analyzed to determine the reaction zero time. In fact, it is well known that when a reacting gas is injected in the reaction zone, some time elapses before the inert gas is purged out of the system and the reactive atmosphere surrounding the sample is established.^[8]

The solid products were examined by XRD with Ni filtered Cu K_α radiation (PHILIPS* PW 1310-01), and

*PHILIPS is a trademark of Philips Electronic Instruments Corp., Mahwah, NJ.

by scanning electron microscopy (SEM 515, Philips Electronic Instruments).

III. THERMODYNAMIC CONSIDERATIONS

A preliminary thermodynamic analysis of the possible reactions that could take place in the Y₂O₃-Cl₂ system was made in order to determine the feasibility of them. When the chlorinating agent is Cl₂, the following reactions are possible:

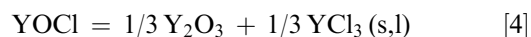
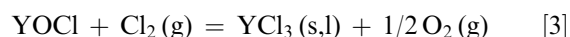
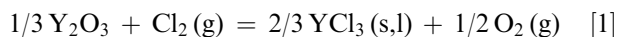


Figure 1 shows the standard Gibbs free energy changes for these reactions. From the analysis of this Ellingham diagram, if the systems were considered to be independent from each other, YOCl has the higher thermodynamic tendency to be produced in all temperatures range studied than the YCl₃. Then the YOCl could be chlorinated (Reaction [3]), or decomposed (Reaction [4]) to give an YCl₃ as a final product (because the Y₂O₃ produced by decomposition will react with Cl₂ to give YCl₃ as a final product as well).

The thermodynamic calculations were performed with the HSC 6.0 Software.^[9] There are insufficient thermodynamic data of YOCl. We have encountered in the literature data at a high temperature range (975 °C to

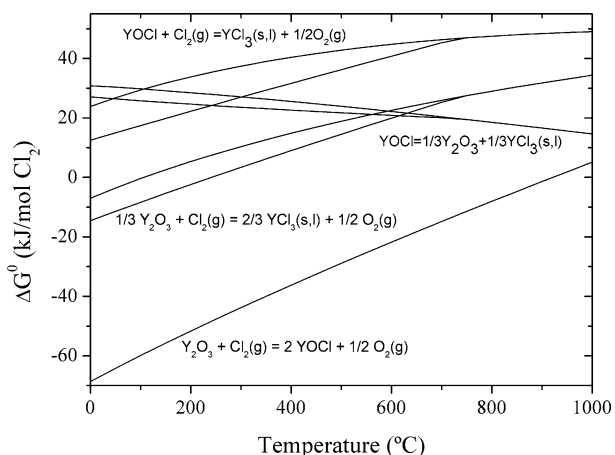


Fig. 1—Standard Gibbs free energy changes (per mole of chlorine) vs temperature for reactions involved in the Y₂O₃-Cl₂ (g) system.

1102 °C)^[10] and at room temperature.^[11,12] Additionally, there is no physical data about this compound. The YOCl data used in the calculations were extrapolated from values reported by Patrikeev.^[10]

IV. RESULTS AND DISCUSSION

A. Nonisothermal Thermogravimetry

Nonisothermal exploratory thermogravimetries were made to determine both the reactivity with temperature and the reaction products of the Y_2O_3 -Cl₂ (g) system. Figure 2 shows the relative mass change vs temperature of the Y_2O_3 in argon-chlorine atmosphere from room temperature to 950 °C. The conditions of the experiment were a heating rate of 3.8 °C/min, an Ar-Cl₂ total flow (Q_{Ar-Cl_2}) of 2 L/h, and a partial pressure of chlorine (p_{Cl_2}) equal to 35 kPa.

A small increase of mass was observed at about 400 °C, showing that the chlorination reaction has started. Two different regions can be seen in the figure, one located between 600 °C to 830 °C with a sharp mass increase, and the other region above 830 °C where a mass loss is observed. The highest value of relative mass change was 0.24. This value corresponds to the mass change involved in Reaction [2]. The solid residue remaining was analyzed by XRD and resulted in 100 pct YOCl, no diffraction lines other than YOCl were observed. Figure 3 shows the XRD patterns for the unreacted Y_2O_3 , the residue after the nonisothermal run, and the YOCl pattern.^[13] From these results, the temperature range chosen was between 575 °C and 950 °C.

B. Isothermal Thermogravimetries

1. Characteristics of the chlorination process

The results were divided in two groups, depending on range of temperature.

(1) 575 °C < T < 800 °C: Figure 4 shows a typical thermogravimetric curve (TG), which corresponds

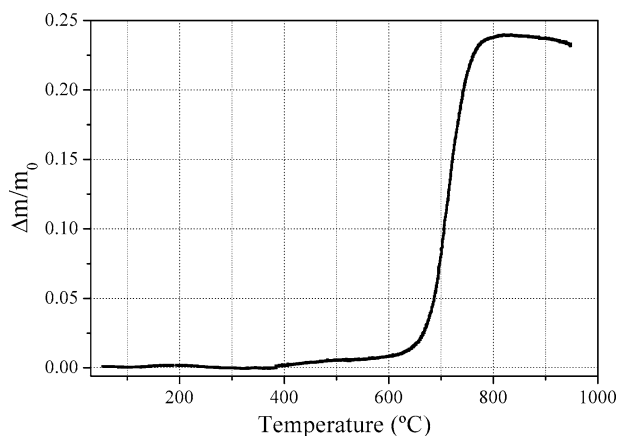


Fig. 2—Nonisothermal thermogravimetry of Y_2O_3 chlorination. Experimental conditions: p_{Cl_2} = 35 kPa, Q_{Ar-Cl_2} = 2 L/h, initial mass = 10 mg, and heating rate = 3.8 °C/min.

to a chlorination of 10 mg of Y_2O_3 performed at 700 °C, p_{Cl_2} 35 kPa, and Q_{Ar-Cl_2} 4 L/h. The curve has sigmoidal shape with three characteristic zones. At the beginning of the reaction, the rate of mass increase is slow until about 400 seconds (zone 1). From this time, the rate suffers an abrupt increase that remains practically linear until about 1500 to 2000 seconds (zone 2). After that, the rate mass change begins to decrease until plateau is reached with a rate of zero (zone 3). The XRD diffractograms of the solid residues of the chlorinations stopped at $\Delta m/m_0$ = 0.05 and 0.13 (indicated as (i) and (ii) in Figure 4) showed the presence of Y_2O_3 and YOCl. The XRD analysis on the final solid product showed only crystalline YOCl.

(2) 800 °C < T < 950 °C: At temperatures above 800 °C, the thermogravimetries show a mass decrease after the higher mass gain. This behavior can be due to two processes: evaporation of YCl_3 produced via the YOCl chlorination through Reaction [3],

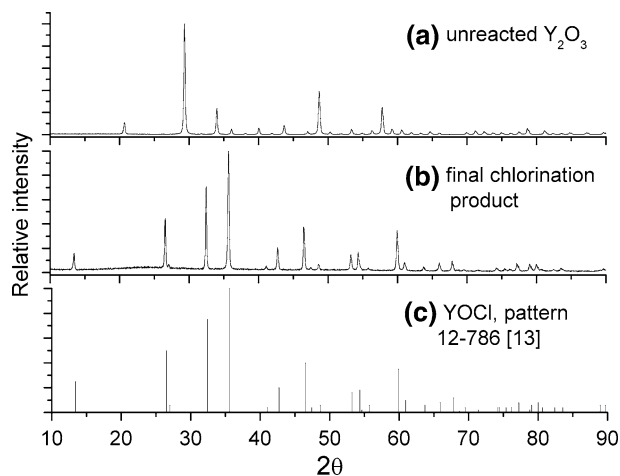


Fig. 3—Diffraction patterns for (a) unreacted Y_2O_3 , (b) reaction product of nonisothermal thermogravimetry, and (c) reference pattern of YOCl^[11].

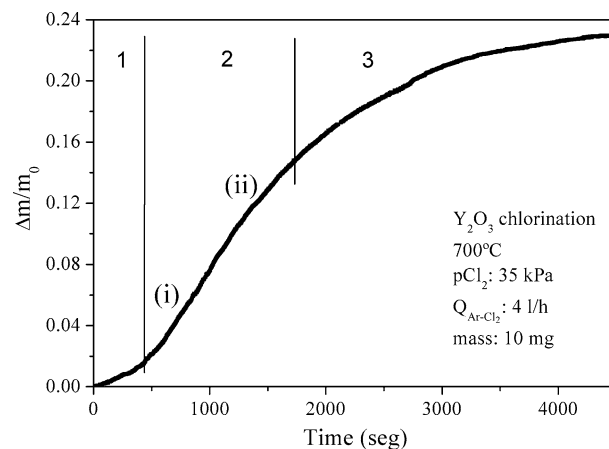


Fig. 4—Typical isothermal thermogravimetry for chlorination of Y_2O_3 at $T < 800$ °C showing characteristic zones (1, 2, and 3). XRD and SEM analyses are indicated by (i) and (ii).

or decomposition/evaporation of the YOCl as can be by Reaction [4]. Yttrium trichloride is a white solid with a temperature of fusion of 721 °C and a boiling point of 1427 °C. The vapor pressure of YCl₃(L) at 800 °C and 950 °C is 7·10⁻⁵ and 2·10⁻³ atm, respectively.^[14]

Figure 5 shows a TG curve for a chlorination performed at 950 °C. The reaction rate is faster than the chlorination at 700 °C, but the shape of the curve is the same. The inset plot on the figure shows the mass loss after the sample reached the higher mass gain. In order to determine if the Cl₂ is responsible for the mass loss, it was suspended. As can be seen, the sample did not suffer any mass change under Ar atmosphere, and it may be interpreted that the mass loss is due to a reaction between YOCl and Cl₂ (Reaction [3]).

The XRD diffractograms of the solid residues at different stages of the reaction were made (they are marked in Figure 5). The results were (i) Y₂O₃ + YOCl, (ii) YOCl, and (iii) YOCl.

C. Effect of the Gas Flow Rate

As reported by several authors,^[15,16] mass transfer into the gas boundary layer surrounding solid samples may play an important role in controlling the reaction rate. For this reason the effect of flow rate at 950 °C and 800 °C was first analyzed. A mass sample of 10 mg was used, and the Cl₂ partial pressure was kept constant at 35 kPa. The experiments were performed at three flow rates: 2, 4, and 8 L/h. Figure 6(a) shows the thermogravimetry performed at 950 °C. It can be seen that as the flow rate was increased, the rate of mass gain was faster. For instance, a relative mass change of 0.15 was achieved in about 68, 41, and 27 seconds for flow rates of 2, 4, and 8 L/h, respectively. Thus, the reaction rate increases with increase of flow rate, and the rate-controlling regime depends on mass transfer in the gaseous phase at 950 °C. Figure 6(b) shows the effect of

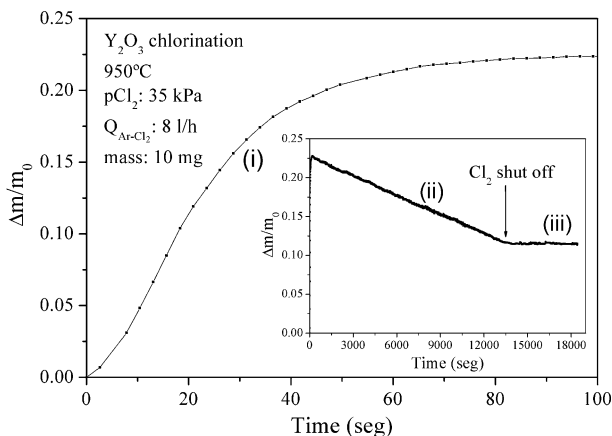
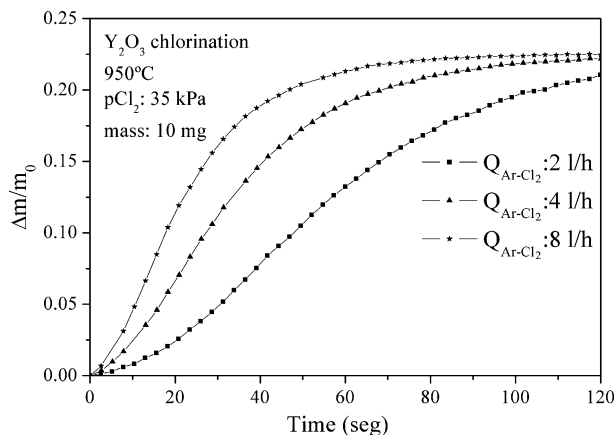
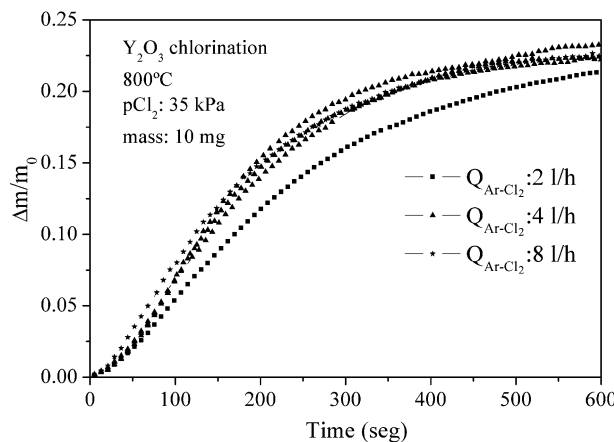


Fig. 5—Typical isothermal thermogravimetry for chlorination of Y₂O₃ at $T > 800$ °C. Right inset plot shows the loss mass stage and the effect of the chlorine shutoff.



(a)



(b)

Fig. 6—Effect of flow rate of Ar-Cl₂ mixture on the chlorination rate of Y₂O₃. Mass sample and chlorine partial pressure were kept constant in all experiments. (a) 950 °C and (b) 800 °C.

the flow rate on the reaction rate at 800 °C. The reaction rate depends on the flow rate for 2 L/h, but it can be seen that for flow rates of 4 and 8 L/h the reaction rate is the same (within the experimental scattering). Figure 6(b) also shows three chlorinations at 4 L/h with the aim of analyzing the reproducibility of the system. It can be seen that the system has good reproducibility in this conditions.

When variations in the flow rate of the reacting gas do not produce significant changes in the reaction rate, it may be concluded that reacting gas starvation is absent. Thus, the thermogravimetry shown in Figure 6(b) permit to conclude that the Ar-Cl₂ flow rate above 4 L/h is high enough for avoiding starvation effects in Y₂O₃ chlorination at 800 °C and p_{Cl_2} 35 kPa. But convective mass transfer through the boundary layer surrounding the sample may play an important role on the overall reaction rate even at a flow rate of 8 L/h. In order to analyze the role of this convective mass transfer, the molar flow of Cl₂ through the boundary layer was estimated by using the Ranz–Marshall equation:^[17,18]

$$N = \frac{D \cdot (2.0 + 0.6 Re^{1/2} Sc^{1/3}) (C_s - C_0) \cdot A}{L} \quad [I]$$

Table I. Comparison between Calculated and Theoretical Molar Flow of Chlorine at Different Temperatures

T (°C)	D (cm/s ²)	ν (cm/s ²)	N Theoretical (mol Cl ₂ /s)*	N_e Experimental (mol Cl ₂ /s) [†]	N/N_e
600	0.76	0.64	5.40×10^{-6}	9.7×10^{-10}	5567
650	0.83	0.71	5.60×10^{-6}	5.2×10^{-9}	1077
700	0.92	0.77	5.90×10^{-6}	2.1×10^{-8}	281
750	1	0.85	6.10×10^{-6}	2.7×10^{-8}	226
775	1.05	0.88	6.15×10^{-6}	8.67×10^{-8}	71
800	1.09	0.92	6.20×10^{-6}	1.3×10^{-7}	48
850	1.18	0.99	6.40×10^{-6}	3.6×10^{-7}	18
900	1.27	1.07	6.60×10^{-6}	4.1×10^{-7}	16
950	1.36	1.15	6.80×10^{-6}	8×10^{-7}	8.5

*Calculated from Eq. [I].

[†]Obtained from the linear range of the thermogravimetric curves.

Conditions used for the calculus: $L = 0.74$ cm, $A = 0.43$ cm², $p_{\text{Cl}_2} = 35$ kPa, and $Q_{\text{Ar-Cl}_2} = 4$ L/h.

where N refers to the molar flow of chlorine; D is the diffusion coefficient for chlorine diffusing through argon; $Re = U \cdot L/\nu$ and $Sc = \nu/D$ represent the Reynolds and Schmidt numbers, respectively (U is the linear fluid velocity and ν is the kinematic viscosity); C_s and C_0 are the chlorine concentrations in the oxide surface and bulk, respectively; A is the sample external surface; and L is the sample characteristic dimension. Table I shows the values of N for $p_{\text{Cl}_2} = 35$ kPa, $Q_{\text{Ar-Cl}_2} = 4$ L/h, and various temperatures as calculated by Eq. [I]. The values of D and ν were obtained from the Chapman/Enskog theory.^[15,19] This table also shows the values of the reaction rate (mol Cl₂/seg) estimated from zone 2 of the thermogravimetric curves and the ratio of the chlorine molar flux theoretical and experimental. The values obtained by using Eq. [I] are only approximate. This equation is valid for a pellet in a freely flowing gas and not for a sample contained within a crucible. Hills^[16] and Hakvoort^[20] concluded that the values given by Eq. [I] are more than one order of magnitude higher than the mass transfer rates into powders contained within crucibles. So it can be seen in the Table I that for temperatures lower than 775 °C the experimental rate is about two orders of magnitude less than the theoretical one, which might indicate that convective mass transfer is not the rate-controlling step.

D. Analysis of Mass Transfer Through the Sample Pores

Mass transfer into the pores of the sample can affect the overall reaction rate. A method for studying the role of mass transfer in powder samples is through the analysis of the effect of the thickness of the reaction bed on the reaction rate. In this work, this analysis was performed by varying the sample mass. The reaction rate decreases as the powder mass increases when the pore diffusion is playing a role in the rate control.

Figure 7 shows thermogravimetric curves obtained by chlorination at 750 °C of samples with different masses contained within a cylindrical crucible, but otherwise keeping the other experimental conditions. The masses used were 2, 4, 10, 20, and 40 mg. As can be seen, the reaction rate does not depend on the sample size at this temperature. Therefore, the mass transfer through the sample pores is not affecting the overall reaction rate.

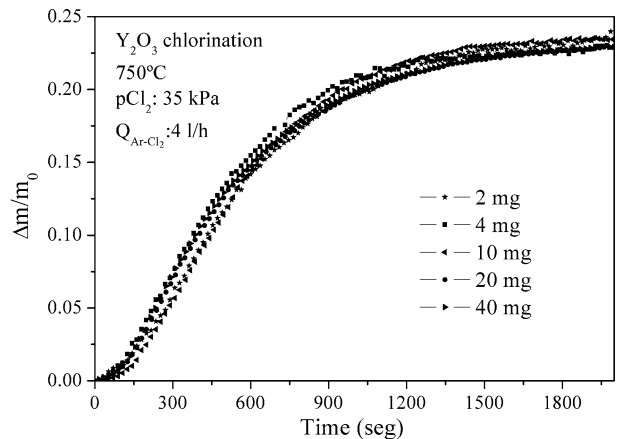


Fig. 7—Effect of sample size on reaction rate of chlorination of Y₂O₃ at 750 °C. Flow rate and chlorine partial pressure were kept constant in all experiments.

E. Determination of the Equation Rate

In a mathematical form for a process controlled by the chemical reaction, the reaction rate (R) can be expressed as a function of T , p_{Cl_2} , and α as follows:

$$R = dx/dt = k(T) \cdot F(p_{\text{Cl}_2}) \cdot G(\alpha) \quad \text{[II]}$$

where $k(T)$ refers to an Arrhenius equation, $F(p_{\text{Cl}_2})$ expresses the dependence of R on p_{Cl_2} , and $G(\alpha)$ is a function that describes the geometric evolution of the reacting solid. The conversion degree is defined as

$$\alpha = \frac{m_t - m_i}{m_i} \cdot \frac{1}{f} \quad \text{[III]}$$

where m_t and m_i refer to the sample mass at a given time and at initial time, respectively, and f is equal to 0.242 (relative mass change of Reaction [2]).

1. Determination of the activation energy

The effect of the temperature on the chlorination of 10 mg of Y₂O₃ by keeping a flow rate of 4 L/h and a p_{Cl_2} of 35 kPa is shown in Figure 8 (575 °C to 800 °C) and Figure 9 (700 °C to 975 °C).

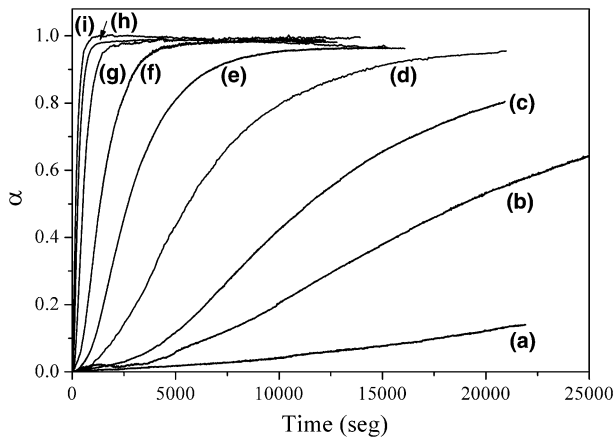


Fig. 8—Effect of reaction temperature ($T < 800\text{ }^{\circ}\text{C}$) on chlorination of Y_2O_3 . Experimental conditions: $p_{\text{Cl}_2} = 35\text{ kPa}$, $Q_{\text{Ar-Cl}_2} = 4\text{ L/h}$, and initial mass = 10 mg. (a) 575 °C, (b) 600 °C, (c) 625 °C, (d) 650 °C, (e) 675 °C, (f) 700 °C, (g) 750 °C, (h) 775 °C, and (i) 800 °C. The stoichiometry considered corresponds to Reaction [2].

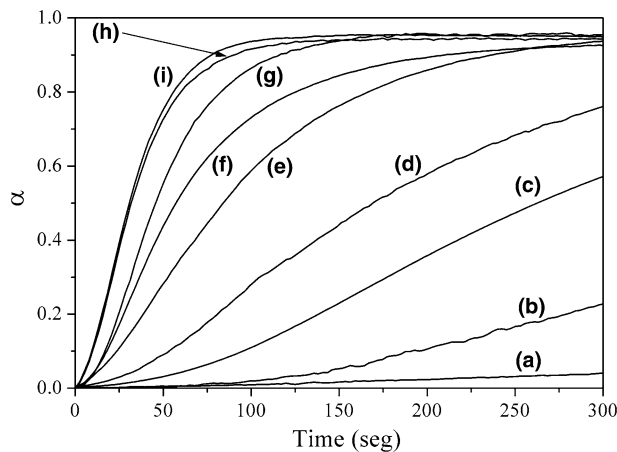


Fig. 9—Effect of reaction temperature (high temperature range) on chlorination of Y_2O_3 . Experimental conditions: $p_{\text{Cl}_2} = 35\text{ kPa}$, $Q_{\text{Ar-Cl}_2} = 4\text{ L/h}$, and initial mass = 10 mg. (a) 700 °C, (b) 750 °C, (c) 775 °C, (d) 800 °C, (e) 850 °C, (f) 900 °C, (g) 925 °C, (h) 950 °C, and (i) 975 °C. The stoichiometry considered corresponds to Reaction [2].

The activation energy (E_a) can be calculated from Eq. [II], even if the functions $F(p_{\text{Cl}_2})$ and $G(\alpha)$ are unknown by applying a “model-free” method.^[21,22] Integrating Eq. [II], assuming that $k(T)$ follows an Arrhenius form, keeping the value of p_{Cl_2} , and applying natural logarithms,

$$\ln t(\alpha) + C(\alpha) + \left(\frac{E_a}{R}\right) \cdot \frac{1}{T} \quad [\text{IV}]$$

where $t(\alpha)$ is the time which the reaction reaches a conversion degree α at a temperature T , R is the gas constant, and $C(\alpha)$ is a function that only depends on α (since p_{Cl_2} is kept constant). The E_a for a given conversion degree is obtained by plotting $\ln t(\alpha)$ vs $1/T$ and calculating the slope of the curve. The analysis of E_a

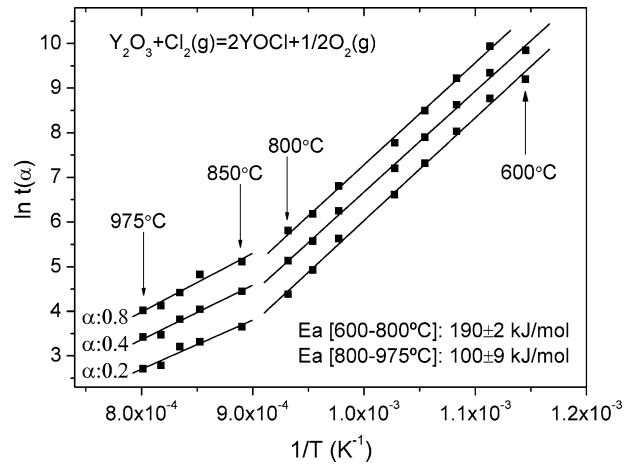


Fig. 10—Plot of $\ln t(\alpha)$ vs $1/T$ (Eq. [IV]) at various conversions for chlorination of Y_2O_3 between 600 °C and 975 °C. The stoichiometry considered corresponds to Reaction [2]. Experimental conditions: $p_{\text{Cl}_2} = 35\text{ kPa}$, $Q_{\text{Ar-Cl}_2} = 4\text{ L/h}$, and initial mass = 10 mg.

at different conversion degrees allows us to determine if there is a unique controlling mechanism in the whole reaction course.

The calculation of the E_a of the formation of YOCl in the 600 °C to 975 °C range is displayed in Figure 10. Between 800 °C and 850 °C, the E_a lines present a change of slope, showing that the kinetic regime is different for $T < 800\text{ }^{\circ}\text{C}$ and for $T > 850\text{ }^{\circ}\text{C}$. The analysis of the effect of the flow rate showed that for $T > 800\text{ }^{\circ}\text{C}$ the reaction rate depends on the flow rate. The values obtained for E_a were $190 \pm 2\text{ kJ/mol}$ for the 600 °C to 800 °C range, and $100 \pm 9\text{ kJ/mol}$ for the 850 °C to 975 °C range. The value calculated for the lower temperature range can be considered an “intrinsic kinetic parameter,” since at these temperatures the reaction rate was not affected by diffusion of Cl_2 through the gas film surrounding the sample and by reaction bed thickness.

2. Effect of chlorine partial pressure

The effect of partial pressure of chlorine was studied at 700 °C in the p_{Cl_2} range of 10 to 70 kPa. The results are shown in Figure 11. To calculate the reaction order of the reaction with respect to p_{Cl_2} the procedure is analogous to that used to determine E_a . Equation [II] is integrated, $F(p_{\text{Cl}_2})$ is assumed that has a form of $B \cdot p_{\text{Cl}_2}^x$ (where B is a constant and x is the reaction order with respect to the p_{Cl_2}), temperature is maintained constant, and natural logarithms are applied. The expression obtained is

$$-\ln t(\alpha) = H(\alpha) + x \cdot \ln p_{\text{Cl}_2} \quad [\text{V}]$$

where $t(\alpha)$ is the time at which the reaction reaches a conversion degree α at a temperature T , and $H(\alpha)$ is a function that depends on α (since T is kept constant). The reaction order for a given conversion degree is obtained by plotting $-\ln t(\alpha)$ vs p_{Cl_2} and calculating the slope of the curve. The inset plot in Figure 11 shows that the reaction order with respect to p_{Cl_2} in the direct

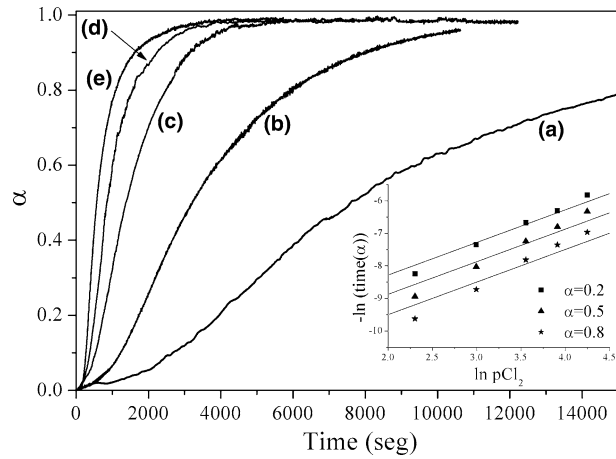


Fig. 11—Effect of chlorine partial pressure on chlorination of Y_2O_3 . Experimental conditions: temperature = 700 °C, $Q_{Ar-Cl_2} = 4$ L/h, and initial mass = 10 mg. (a) 10 kPa, (b) 20 kPa, (c) 35 kPa, (d) 50 kPa, and (e) 70 kPa. Right inset plot shows lineal fit obtained from Eq. [V].

chlorination of Y_2O_3 is 1, and the chlorination rate is proportional to pCl_2 .

3. Reaction model—determination of $G(\alpha)$

The sigmoidal shape of the thermogravimetric curves is characteristic of a “nucleation and growth reaction model.” An analysis of the evolution of the solid through the reaction confirms the application of this model. In Figure 12(a) a SEM image of a particle of the initial oxide is shown. It has an irregular shape with sharp angles. The surface is quite smooth with a considerable number of cracks. By XRD it is known that after chlorination a new phase (YOCl) is presented. At any temperature, little regions appear on the partially reacted particle surface and they have a different morphology than before, covering a fraction of the surface (Figures 12(b) and (c)). However, when reaction degree advances both samples show that the YOCl nuclei were grown in the overall volume of the initial oxide and well defined crystals are observed (Figures 12(d) through (f)). This type of crystal growth is in agreement with the Johnson-Mehl-Avrami (JMA) model,^[23–26] which is proposed to be considered. The growth of the YOCl nuclei is anisotropic, because they are not spherical but face-rounded cylinders.

The EDS results of the samples of Figure 12 are shown in Table II. It can be seen that for the partially reacted samples the mean molar fractions of Y and Cl are 65.5 and 34.5 pct for the sample reacted at 700 °C ($\alpha = 0.55$) and 70 and 30 pct for the sample reacted at 900 °C ($\alpha = 0.58$). These results are in good agreement with those expected for the theoretical molar fractions of Y_2O_3 and YOCl for this reaction degree (64 pct Y-36 pct Cl, for $\alpha = 0.56$). The EDS analysis carried out on the samples completely reacted were 54 pct Y-46 pct Cl and 52 pct Y-48 pct Cl for the samples chlorinated at 700 °C and 950 °C, respectively. The molar fractions expected for these samples are 50 pct Y and 50 pct Cl, since they are 100 pct YOCl.

Therefore, the α - t curves can be analyzed with the Johnson-Mehl-Avrami description,^[23–26] which gives for isothermal transformations

$$\alpha = 1 - \exp[-K(T) \cdot t]^n \quad [VI]$$

with n as the JMA exponent and the reaction rate constant $K(T)$ given by

$$K = K_0 \cdot \exp\left(-\frac{Ea}{R \cdot T}\right) \quad [VII]$$

where K_0 is the pre-exponential factor and Ea is the effective Ea .

The JMA kinetic parameters K_0 , n , and Ea depend on the nucleation and growth mechanism. In principle, for isokinetic transformations^[27] n can only take specific values arising from the different nucleation models (continuous nucleation and site saturation) and K_0 and Ea are independent of temperature. However, Kempen^[28,29] has proven (numerically) that intermediate and temperature dependent values of the JMA kinetic parameters are also possible for mixtures of the different nucleation models.

The isothermal α - t curves were fitted with Eq. [VI] in a nonlinear way. Activation energy was obtained by an Arrhenius plot of the values of K calculated at the different temperatures (Figure 13). As expected, the curve has a change in the slope for temperatures higher than 850 °C, indicating that there is a change in the rate-controlling step. The values calculated were 187 ± 3 kJ/mol in the 600 °C to 800 °C range, and 105 ± 11 kJ/mol in the 850 °C to 975 °C range. These values are in good agreement with those obtained by the isoconversional method (190 ± 2 and 100 ± 9 kJ/mol, respectively).

The mean value estimated for n was 1.51 ± 0.14 . This value can be understood taking into account that the transformation reaction has diffusion-controlled growth and the shape of the growing particles is anisotropic (Figures 12(d) through (f)). On the basis of the work of Kempen *et al.*^[28,29] for diffusion control growth, the value of n varies (1) between 1/2 (one-dimensional growth) and 3/2 (three-dimensional growth) for site saturation and (2) between 3/2 (one-dimensional growth) and 5/2 (three-dimensional growth) for continuous nucleation. Therefore, an n value of 1.51 is compatible with anisotropic growth, which is rate controlled by diffusion.

Finally, from Eqs. [II] and [VI]

$$\begin{aligned} G(\alpha) &= n \cdot (1 - \alpha) \cdot [-\ln(1 - \alpha)]^{(n-1)/n} \\ &= 1.51 \cdot (1 - \alpha) \cdot [-\ln(1 - \alpha)]^{0.34} \end{aligned} \quad [VIII]$$

V. CONCLUSIONS

The direct chlorination of yttrium oxide in the temperature range of 575 °C to 975 °C leads to the formation of yttrium oxychloride as the reaction product in an initial stage. For temperatures above 800 °C, the yttrium oxychloride is chlorinated to yttrium

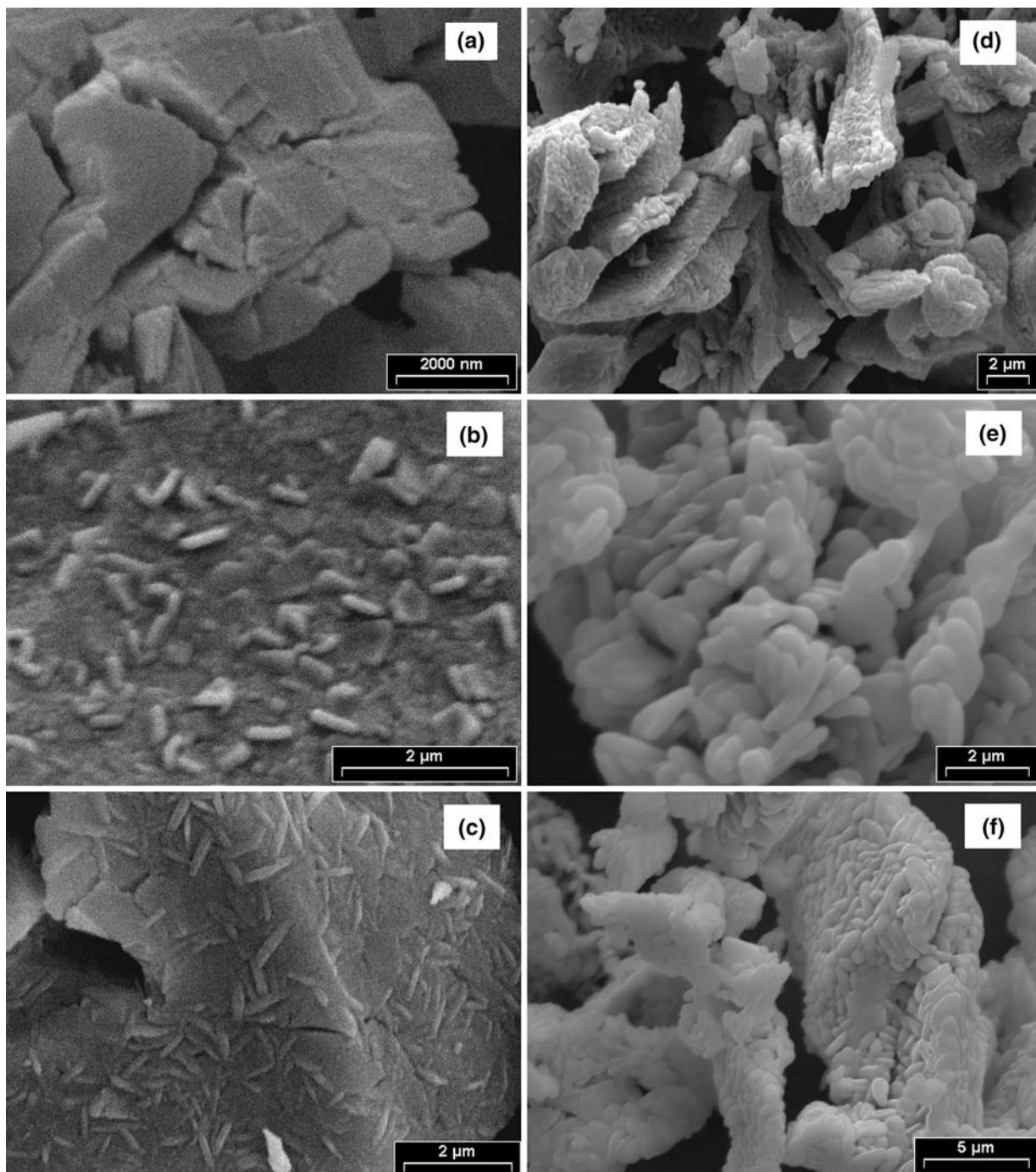


Fig. 12—SEM images of samples at different reaction stages. (a) initial yttrium oxide; (b) $\alpha = 0.55$, 700 °C; (c) $\alpha = 0.58$, 900 °C; (d) $\alpha = 1$, 700 °C; (e) and (f) $\alpha = 1$, 950 °C.

trichloride, which is evaporated. On the basis of the kinetics and morphological results, the chlorination is controlled by the chemical processes below 800 °C, while at higher temperatures, the reaction rate depends on the reactive gas flow rate. The α - t curves were analyzed with the Johnson–Mehl–Avrami description for nucleation and growth transformations. The calculated α - t curves showed good agreement with the

experimental data and provided a good description of the reaction kinetics with $n \sim 1.5$, which could correspond to diffusion rate control for anisotropic phase growth.

From the values of the rate constants calculated at different temperatures, activation energies of 187 ± 3 and 105 ± 11 kJ/mol were obtained in the temperature ranges of 575 °C to 800 °C and 850 °C to 975 °C,

Table II. EDS Results of the Samples of Figure 12

Sample	EDS Results (At. Pct)	
	Y	Cl
Initial oxide (Fig. 12(a))	100	—
700 °C, $\alpha = 0.55$ (Fig. 12(b))	65.5	34.5
700 °C, $\alpha = 1$ (Fig. 12(d))	54	46
900 °C, $\alpha = 0.58$ (Fig. 12(c))	70	30
950 °C, $\alpha = 1$ (Figs. 12(e) and (f))	52	48

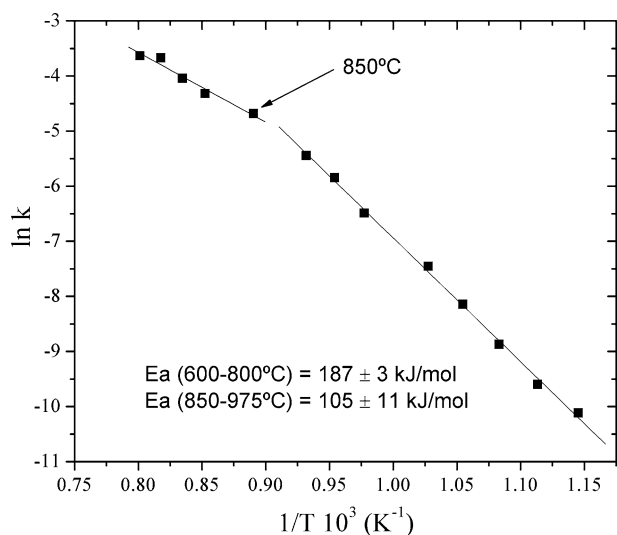


Fig. 13—Arrhenius plot of rate constants obtained from JMA analysis. Stoichiometry considered corresponds to Reaction [2]. Experimental conditions: $p_{Cl_2} = 35$ kPa, $Q_{Ar-Cl_2} = 4$ L/h, and initial mass = 10 mg.

respectively. The isoconversional method showed that the reaction mechanism is the same at the overall reaction and the values of activation energies obtained were 190 ± 2 at 575 °C to 800 °C and 100 ± 9 kJ/mol at 850 °C to 975 °C, which are very close to those calculated from the Johnson–Mehl–Avrami description. The effects of parameters studied in this system could be expressed by a global reaction rate equation, as follows:

$$R = dx/dt = 10^5 \text{ kPa}^{-1} \cdot \exp\left(-\frac{187 \text{ kJ}\cdot\text{mol}^{-1}}{R\cdot T}\right) \cdot p_{Cl_2} \cdot 1.51 \cdot (1 - \alpha) \cdot [-\ln(1 - \alpha)]^{0.34}$$

ACKNOWLEDGMENTS

The authors thank the Agencia Nacional de Promoción Científica y Tecnológica (ANPCyT), Consejo Nacional de Investigaciones Científicas y Técnicas (CONICET), and Universidad Nacional del Comahue for the financial support of this work.

REFERENCES

1. M. Gimenes and H. Oliveira: *Metall. Trans. B*, 2001, vol. 32B, pp. 1007–13.
2. F.H. Spedding: in *Handbook on the Physics and Chemistry of Rare Earths*, K.A. Gschneider, Jr. and L. Eyring, eds., North-Holland, Amsterdam, 1978, p. 15.
3. G. Morteani: *Eur. J. Mineral*, 1991, vol. 3, pp. 641–50.
4. C.K. Gupta and N. Krishnamurthy: *Int. Mater. Rev.*, 1992, vol. 37 (5), pp. 197–248.
5. E. Augusto and H. Oliveira: *Metall. Mater. Trans. B*, 2001, vol. 32B, pp. 785–91.
6. A.I. Braginski, A.O. Isenberg, M.T. Miller, and T.R. Oeffinger: *Ceram. Bull.*, 1972, vol. 51 (8), pp. 630–32 and 636.
7. D.M. Pasquevich and A.M. Caneiro: *Thermochim. Acta*, 1989, vol. 156, pp. 275–83.
8. H.S. Ray: *J. Therm. Anal.*, 1990, vol. 36, pp. 743–64.
9. HSC 6.1, Outokumpu Research Oy, Pori, Finland.
10. Y.B. Patrikeev, G.I. Novikov, and V.V. Badovskii: *Russ. J. Phys. Chem.*, 1973, vol. 47 (2), p. 284.
11. V.S. Yungman, V.P. Glushko, V.A. Medvedev, and L.V. Gurvich: *Thermal Constants of Substances*, Wiley, New York, NY, 1999.
12. H. Oppermann, S. Ehrlich, and C. Hennig: *Z. Naturforsch., Bi: Chem. Sci.*, 1997, vol. 52 (3), pp. 305–10.
13. Joint Committee for Powder Diffraction Standards, Powder Diffraction File, International Center for Diffraction Data, Swarthmore, PA, 1996 (card number 120786).
14. I. Barin: *Thermochemical Data of Pure Substances*, VCH Verlags Gesellschaft, Weinheim, 1993.
15. J. Szekeley, J.W. Evans, and H.Y. Sohn: *Gas-Solid Reactions*, Academic Press, New York, NY, 1976, chap. 2, pp. 10–22.
16. A.W.D. Hills: *Metall. Trans. B*, 1978, vol. 9B, pp. 121–28.
17. W.E. Ranz and W.R. Marshall, Jr.: *Chem. Eng. Prog.*, 1952, vol. 48 (3), pp. 141–46.
18. W.E. Ranz and W.R. Marshall, Jr.: *Chem. Eng. Prog.*, 1952, vol. 48 (4), pp. 173–80.
19. G.H. Geiger and D.R. Poirier: *Transport Phenomena in Metallurgy*, Addison-Wesley, Massachusetts, MA, 1973, chap. 1, pp. 7–13.
20. G. Hakvoort: *Thermochim. Acta*, 1994, vol. 233, pp. 63–73.
21. J.H. Flynn: *J. Therm. Anal.*, 1988, vol. 34, pp. 367–81.
22. S. Vyazovkin: *Thermochim. Acta*, 2000, vol. 355, pp. 155–63.
23. M. Avrami: *J. Chem. Phys.*, 1939, vol. 7 (12), pp. 1103–113.
24. M. Avrami: *J. Chem. Phys.*, 1940, vol. 8 (2), pp. 212–24.
25. M. Avrami: *J. Chem. Phys.*, 1941, vol. 9 (2), pp. 177–84.
26. W.A. Johnson and R.F. Mehl: *Trans. Am. Inst. Min. Metall. Eng.*, 1939, vol. 135, pp. 416–27.
27. J.W. Christian: *The Theory of Transformations in Metals and Alloys*, Pergamon Press, Oxford, United Kingdom, 1965, chap. 12, pp. 525–48.
28. A.T.W. Kempen, F. Sommer, and E.J. Mittemeijer: *J. Mater. Sci.*, 2002, vol. 37 (2), pp. 1321–32.
29. A.T.W. Kempen, F. Sommer, and E.J. Mittemeijer: *Acta Mater.*, 2002, vol. 50 (14), pp. 1319–29.